Trapping of Metallic Porphyrins by Asphaltene Aggregates: A Size Exclusion Microchromatography With High-Resolution Inductively Coupled Plasma Mass Spectrometric Detection Study

ARTICLE *in* ENERGY & FUELS · JULY 2012

Impact Factor: 2.79 · DOI: 10.1021/ef3002857

6 AUTHORS, INCLUDING:

Socrates Acevedo
Central University of Venezuela
111 PUBLICATIONS **1,269** CITATIONS
SEE PROFILE

Brice Bouyssiere
Université de Pau et des Pays de l'Adour
50 PUBLICATIONS **639** CITATIONS
SEE PROFILE

energy&fuels

Article

pubs.acs.org/EF

Trapping of Metallic Porphyrins by Asphaltene Aggregates: A Size Exclusion Microchromatography With High-Resolution Inductively Coupled Plasma Mass Spectrometric Detection Study

Sócrates Acevedo,*[,†] Karina Guzmán,[†] Henry Labrador,[‡] Herve Carrier,[§] Brice Bouyssiere,[∥] and Ryszard Lobinski[∥]

[†]Universidad Central de Venezuela, Facultad de Ciencias, Escuela de Química, Caracas, 1053, Venezuela

[‡]Universidad de Carabobo, Facultad Experimental de Ciencias y Tecnología, Departamento de Química, Valencia, Edo. Carabobo, Venezuela

[§]Laboratoire des Fluides Complexes, Universite de Pau et des Pays de l'Adour, UMR 5150, BP 1155, F-64013 Pau, France

[∥]CNRS/UPPA, Laboratoire de Chimie Analytique Bio-inorganique et Environnement, UMR 5254, Helioparc, 2, Av. Pr. Angot, F-64053 Pau, France

ABSTRACT: A combined liquid chromatography coupled to a mass spectrometer with an ICP detector (μSEC-HR ICP MS; μSEC ICP for brevity) technique was used to analyze the metals in four asphaltenes and their corresponding A1 (toluene insoluble), A2 (toluene soluble), and trapped compound (TC, heptane soluble) fractions. For three of the asphaltene samples, the normalized μSEC ICP profiles for both nickel and sulfur were very similar, showing that nickel porphyrins were distributed in almost all types of asphaltene aggregates. Extensive overlapping with sulfur profiles was observed for all vanadium and nickel profiles at retention times below the maximum bands. This suggests that large amounts of nickel and other organometallic or metal-porphyrin-type (MP) compounds are interlocked with asphaltene molecules, forming aggregates in solution. The separation of MP compounds using common separation techniques is very difficult as extraction would require dissociation into several molecules. The presence of TCs (e.g., compounds other than asphaltenes that are soluble in *n*-heptane) in asphaltene aggregates was related to the fractal structure of asphaltene aggregates in which voids are filled with components coming from the surrounding media. Apparently, complete trapping of TCs is achieved by performing aggregate rearrangement after penetration, leading to an aggregate structure in which the TCs remain trapped. A similar trapping mechanism is proposed herein for the MP compounds. Accordingly, no covalent bonds or specific interactions appear to be required to account for the presence of MPs within asphaltene aggregates.

INTRODUCTION

The negative impact of vanadium and nickel on crude oil processing as well as the increasing use of heavy and extra-heavy oils as a result of dwindling light oil reserves has promoted a significant research effort aimed at finding ways of removing or separating these contaminants from crude oil and related products. A recent review on this and other relevant topics is available.[1] Metal porphyrins (MP) are known to concentrate in the heavy, more polar fractions of crude oil and, particularly, in the asphaltene fraction.[1,2] This association with asphaltenes is probably the reason behind the great difficulties in extracting or separating MPs from crude oils or residues. Although the association of MPs with asphaltenes is well documented,[1−3,7−14] there is no general agreement on the mechanisms of such associations. The trapping of MPs by asphaltenes was predicted a long time ago when the presence of free radicals in asphaltenes was first discussed.[3] In later studies, we proposed that the presence of free radicals (very reactive species) in asphaltenes was possible because they were present within asphaltenes aggregates, thus insulating them from the environment. This concept can be also used for trapping MPs, to obtain geochemical markers,[4,5] and to detect paraffins[6] and occluded matter[7] in asphaltenes.

In a series of papers, van Berkel et al. reported the use of both electron ionization mass spectrometry (EIMS)[8,9] and electron ionization tandem mass spectrometry (EIMS/MS)[10] to study VO(II) and Ni(II) compounds in a New Albany bitumen and a pyrolysate obtained from kerogen of the shale derived from the same location. Their results indicated that both the bitumen and the pyrolysate contained vanadyl porphyrins of similar structure. They also concluded that the appearance of porphyrins in the pyrolysate was produced by an enhanced solubilization/desorption mechanism rather than by C−C bond scission and, consequently, that metalloporphyrins are held in the asphaltene/kerogen matrix by association rather than by chemical bonding.[10]

Qian et al. used atmospheric pressure photoionization (APPI) coupled to Fourier transform ion cyclotron resonance-mass spectrometry (FTICR-MS) to analyze an asphaltene sample, in which they found the characteristic Z-distribution of VO porphyrins (Z-number range, −28 to −54), which suggests involvement of benzene and naphthenic moieties in the growth of porphyrin ring structures[11,12] (see the Nomenclature section for a Z definition). Z-numbers of −40, −42, and −44 are consistent with naphthenic rings condensed to tetrapyrrolic

Received: February 16, 2012
Revised: July 2, 2012
Published: July 9, 2012

porphyrin systems.[12] Taking these Z-values into consideration, a more extended aromatic condensation is expected . These aromatic groups would increase the affinity between MPs and asphaltenes. Using a similar MS technique, the same research group studied nickel porphyrins in a nickel-enriched asphaltene sample with a low sulfur content (to diminish possible interference with sulfur compounds showing very similar molecular mass, MM).[12] The structure assignment, complemented with a Ni isotope distribution, was consistent with nickel porphyrins containing from 26 to 41 carbon atoms and with Z-numbers between −26 and −44 (MM between 462 and 630 g mol^{-1}). A similar Z-distribution was found for VO porphyrins. Etio and DPEP types were the most abundant, showing small quantities of large negative Z-values. No nickel or VO compounds other than porphyrins were reported using a very high resolving (HR) power (over 500 K) MS technique.[12]

Grigsby and Green analyzed a vanadium-enriched fraction from the >700 °C residue of Cerro Negro using a low-eV HR/MS method. The presence of Etio, DPEP, and other vanadyl porphyrins with MMs ranging from 487 to 867 was reported. The authors concluded that at least a part of the apparent nonporphyrinic vanadium thought to be present in the fraction was, in fact, porphyrinic.[13]

X-ray absorption fine structure (XAFS) spectroscopy and X-ray absorption near-edge structure (XANES) results led Goulon et al. to conclude that all the vanadium present in Boscan asphaltenes was tetra-coordinated to four nitrogen atoms (i.e., all the vanadium was bound to porphyrins).[14] This result is in agreement with reports by Miller et al.[15]

The Marshall group identified a series of etio and DPDP vanadyl porphyrins in a South American heavy oil using APPI-FTICR-MS techniques.[16] These authors reported an MM distribution ranging from about 473 to 697 g mol^{-1} and from 485 to 723 g mol^{-1} for etio and DPEP vanadyl porphyrins, respectively. Since the number of double bond equivalents (DBE) was the same for each series, substantial alkyl substitution is required to reach these high MMs (16 and 17 CH_2 to cover the etio and DPEP MM ranges). Thus, these high MM vanadyl porphyrins are expected to have high solubility in the oil.

The aggregation between asphaltene models and metal porphyrins (e.g., vanadyl and nickel) was analyzed by Yin et al. by means of simulation experiments.[17] No evidence of aggregation was found by fluorescence methods in *n*-heptane solutions containing nickel and vanadyl porphyrins along with oxygen- and sulfur-containing compounds such as dibenzofuran and dibenzothiophene. Specific interactions between sulfur- or oxygen-containing compounds with either nickel or vanadyl porphyrins were not found when performing this study. However, in our opinion, intermolecular interactions in general cannot be ruled out with simplistic simulation of asphaltenes aggregation. A realistic simulation of this process would require mixtures of models capable of mimicking aggregate formation in most solvents (see the Discussion). These authors also propose that for the non-Soret petroporphyrins to bind properly, the tetrapyrrole ring system must be covalently attached to other structures in order to enhance the binding to the asphaltene components by additional interactions such as hydrogen-bonding and acid−base interactions. The above reports[11,12] are partially consistent with this statement as large and negative Z-numbers typical of structures containing polyaromatic rings were suggested.[12] However, no functional groups capable of hydrogen-bonding interactions were reported by Quian et al.[11,12]

With the aim of searching for specific interactions between asphaltenes and metallic porphyrins [Ni(II) and VO(II)], Kovalenko et al. used quantum mechanics methods to support both axial and hydrogen-bonding interactions.[18] In this sense, hydrogen bonding between a ring C−H type hydrogen in pyridine and VO was proposed. However, such interactions are expected to be very weak and, consequently, they are unlikely to account for the above MP−asphaltene aggregation in most solvents.

Asphaltenes have a strong aggregation tendency even when dissolved in very good solvents and under high-temperature conditions. For instance, the RED value between asphaltene and *o*-dichlorobenzene is very low, which unambiguously places this solvent among the best for asphaltenes.[19] However, asphaltene and its A1 and A2 fractions form aggregates in this solvent even at 130 °C.[20] The A1 fraction was found to have the highest aggregation tendency when dissolved in *o*-dichlorobenzene and other solvents (e.g., nitrobenzene, chloroform, toluene).[20] M_n values ranging from 4000 to 7000 g mol^{-1} were reported for several asphaltene samples dissolved in tetrahydrofuran (THF).[21] According to recent reports, the average MM should be around 800 g mol^{-1}.[22,23] Hence, asphaltene aggregation is expected to occur in the μSEC experiments described below, as they were carried out in THF at room temperature. According to the values indicated above, these aggregates may contain five or more molecules.

A fractal structure based on interlocking of asphaltene molecules in their aggregates was proposed by Sheu, based on conductivity measurements.[24] These measurements were

Table 1. Concentrations in THF Solution of Different Samples Used in This Work[a]

sample	g kg^{-1}	g L^{-1}
Furrial	9.85	8.76
Furrial A2	9.79	8.70
Furrial A1	10.03	8.92
Furrial TC	84.8	75.39
CN As	10.23	9.09
CN A2	9.99	8.88
CN A1	9.91	8.81
CN TC	9.81	8.72
Boscan	9.72	8.64
Boscan A1	10.05	8.93
Boscan A2	9.94	8.84
Boscan TC	9.83	8.74
French	9.75	8.67
French A1	10.02	8.91
French A2	9.63	8.56
French TC	9.98	8.87

[a]THF density = 0.89 g L^{-1} at 20 °C.

Table 2. Fractions Recovered[a] and Percentage of Different Fractions for the Four Samples Studied

	percentage of fraction in sample (*f*)			
fraction	French	Boscan	CN	Furrial
A1	9	49	56	49
A2	79	47	39	38
TC	11	4	5	13
recovery (*R*)	80	90	80	80

[a]With respect to asphaltenes recovered; 10−20% estimated errors.

dx.doi.org/10.1021/ef3002857 | *Energy Fuels* 2012, 26, 4968−4977

Table 3. Metal Concentrations in Asphaltenes and Fractions[a]

	metal/mg kg^{-1}							
	^{51}V	^{58}Ni	^{60}Ni	^{98} Mo	^{206}Pb	^{208}Pb	^{118}Sn	V/Ni
Cerro Negro Samples								
asphaltenes	1347	217	213	8	18	20	0	6
A1	1639	242	235	3	13	14	10	7
A2	1432	229	219	4	18	18	0	6
TC	510	30	30	0	8	9	0	17
Furrial Samples								
asphaltene	845	164	163	5	21	22	3	5
A1	760	144	145	0.3	9	10	0.3	5
A2	600	91	95	0.5	16	17	0.18	6
TC	45	≈0	≈0	0	10	0.6	0	

[a]A 5−10% error estimated for V and Ni; no error was estimated for other metals.

Table 4. Percentage Distributions of V and Ni[a] among Different Fractions of Asphaltenes

	CNAs		Furrial	
fraction	V	Ni	V	Ni
A1	61	60	61	66
A2	37	40	38	34
TC	2	1	1	0

[a]%$M(i)$: see text and eq 4; errors of about 30% (A1), 25% (A2), and 20% for TC were estimated from the uncertainties in metal content (M_i), fraction percentage (f_i), and error propagation.

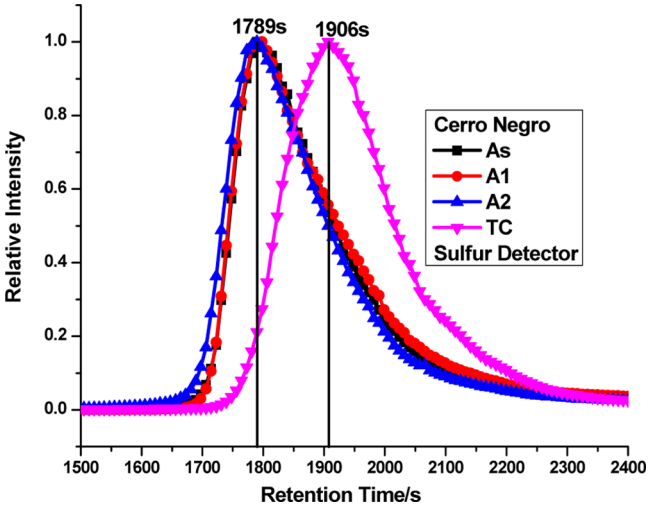

Figure 1. Normalized μSEC ICP sulfur profiles for Cerro Negro asphaltenes and corresponding fractions A1, A2, and TC. These have similar profiles showing no relevant difference in either chemical composition or size. Relatively low retention time and shift of profile to the right are observed for the TC fraction.

consistent with housing of HCl drops in the expected cavities of the fractal-like asphaltene aggregates. Obviously, as mentioned above,[3−6] this approach is consistent with the trapping of compounds other than asphaltenes inside fractal cavities or voids (see below).

EXPERIMENTAL SECTION

Materials. Boscan, Cerro Negro, and Furrial crude oils with API gravities of 10.3, 8.5, and 21, respectively, were obtained from PDVSA. The French crude oil sample (saturates, 19%; aromatics, 64%; resins, 12%; asphaltenes, 5%) was obtained from the Total Oil Company. Asphaltenes were obtained after addition of excess *n*-heptane to the crude oil, following reported procedures.[25] A thorough Soxhlet extraction with boiling *n*-heptane was employed to remove as much resins as possible, as previously reported.[6]

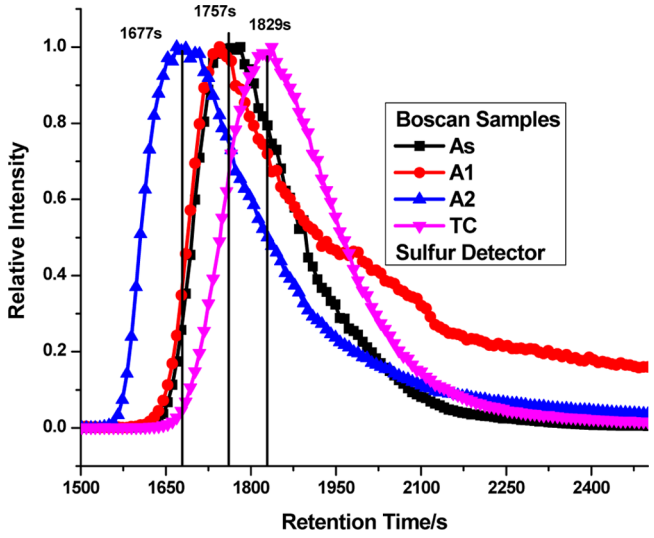

Figure 2. Normalized μSEC ICP profile corresponding to Boscan samples registered with a sulfur detector. As was the case for Cerro Negro (Figure 1) the band corresponding to TC is shifted to the right.

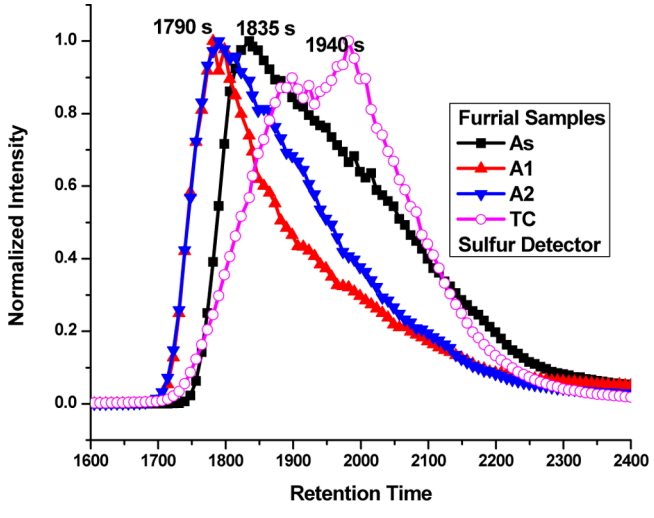

Figure 3. Comparison of normalized μSEC ICP for Furrial asphaltene samples; differences in profiles are likely the consequence of differences in chemical composition. As was the case for others (Figures 1 and 2), the TC band is shifted to the right.

dx.doi.org/10.1021/ef3002857 | *Energy Fuels* 2012, 26, 4968−4977

A1 (very low solubility in toluene; around 90 mg L^{-1}; room temperature), A2 (toluene solubility similar to asphaltenes), and TC (soluble in *n*- heptane) fractions were isolated using the reported *p*-nitrophenol (PNP) method.[6] Briefly, asphaltenes were dissolved (8 g L^{-1}) in a cumene (isopropylbenzene) solution saturated with PNP under ambient conditions. After 3 d (Cerro Negro and Furrial samples), the A1-PNP precipitated solid complex was filtered and treated (dissolution in chloroform, followed by extraction with aqueous sodium hydroxide) for total removal of PNP, generating the A1 fraction. The filtrate, containing A2, TC, and PNP, was treated with three volumes of *n*-heptane, which led to a precipitated solid (A2 + PNP) along with a solution (TC + PNP). Both components were then treated as indicated above for PNP removal. In the case of Boscan asphaltenes, it was necessary to boil the asphaltene−cumene solution saturated with PNP for 72 h to obtain precipitation of the PNP−A1 complex. In the case of the French sample, 1 month of contact time was required for the separation of the A1 complex. Unless otherwise stated, the isolation procedure was the same as that described above. Thus, TC involves a fraction soluble in *n*-heptane, which remains in the asphaltenes after the above thorough Soxhlet extraction with *n*-heptane.

Methods. *Inductively Coupled Plasma Mass Spectrometry (ICP MS) Detection.* The detailed conditions used for ICP MS detection have been previously reported,[26] and a summarized description is given below. A Thermo Scientific Element XRsector field ICP MS instrument operated at a resolution of 4000 (medium resolution) was used to access spectrally interfered isotopes of ^{60}Ni, ^{32}S, and ^{51}V. The spectrometer was equipped with a Fassel-type quartz torch shielded with a grounded Pt electrode and a quartz injector (1.0 mm i.d.). A Pt sampler (1.1 mm orifice diameter) and a Pt skimmer (0.8 mm orifice diameter) were used. An O_2 flow was continuously supplied to the nebulizer Ar gas flow. The mass spectrometer was fitted with a modified DS-5 microflow total consumption nebulizer (CETAC, Omaha, NE) mounted on a laboratory-made low-volume (8 mL) single-pass jacketed glass spray chamber without a drain, as described elsewhere.[27] The spray chamber was thermostatted to 60 °C with a water−glycol mixture using a Neslab RTE-111 (Thermo Fisher Scientific, Waltham, MA) temperature-controlled bath circulator. The carrier solution in the microflow injection (μFI) and the mobile phase in μSEC experiments were delivered using a Dionex (Amsterdam, The Netherlands) HPLC system comprising an UltiMate 3000 microflow pump, an UltiMate 3000 autosampler, and a low port-to-port dead-volume microinjection valve.

Chromatography and ICP MS Detection. Separations were carried out using three Shodex microtype styrene−divinylbenzene gel permeation columns (0.1 mm i.d., 250 mm length): KF402-1E. ICP MS conditions were optimized daily using a 1.0 ng g^{-1} multielement tuning solution delivered via a syringe pump. The peaks of the isotopes chosen at these conditions were baseline resolved from the interferences. μFI-ICP MS and μSEC-ICP MS were carried out in the time-resolved mode. A built-in software application was used to integrate the signal recorded. The data acquisition method was updated with a mass offset determined for each isotope in order to compensate for the mass drift coming from the magnet sector.

The following method was used to estimate the amounts of vanadium compounds dissociated from asphaltenes during μSEC runs. We defined this as dissociated vanadium or DV (see below). This parameter was determined from the normalized μSEC ICP profiles registered with sulfur and vanadium detectors by subtracting the area under the corresponding bands, as show in eq 1:

$$\%\mathrm{DV} = 100\left(\frac{A_V - A_S}{A_S}\right) \quad (1)$$

where A_V and A_S refer to areas under the profile measured with vanadium and sulfur detectors, respectively. Sulfur was assumed to be present in the entire asphaltene sample.

RESULTS

The concentrations of the samples injected in the μSEC column are shown in Table 1. These concentrations were selected for detection convenience and only in one case (Furrial TC) was a much higher concentration. Typical concentrations were fixed at around 9.9 g kg^{-1} in order to ensure the presence of aggregates.

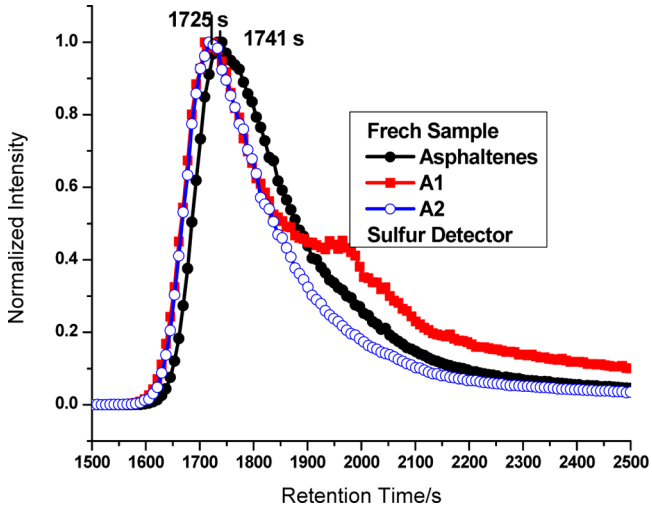

Figure 4. Comparison of normalized μSEC ICP profiles for French asphaltenes samples. Samples A1 and A2 have the same retention time equal to 1725 s.

Table 5. Retention Times of Samples Measured Using μSEC ICP Employing a Sulfur Detector

	retention time/s[a]			
sample	asphaltene	A1	A2	TC
French	1733	1725	1725	
Boscan	1765	1740	1685	1829
Cerro Negro	1789	1789	1789	1906
Furrial	1831	1790	1790	1940

[a]Corresponding to the band maximum.

The percentage of recovered material, *R*, and the percentage of fractions from asphaltene fractionation with PNP are shown in Table 2 and were calculated using eqs 2 and 3:

$$R = 100\left(\frac{m_R}{m_0}\right) \quad (2)$$

$$f = 100\left(\frac{m_f}{m_R}\right) \quad (3)$$

In these equations, *f* represents the percentage of each fraction; m_R is the total mass recovered (mass of A1 + A2 + TC); m_0 refers to the initial mass of asphaltene; and m_f is the recovered mass of each fraction. The recovery of samples was satisfactory, although somewhat low because of manipulation during work up. For these *R* and *f* values, typical errors ranged between 10 and 20%.

The isolation of fractions A1 and A2 was previously reported for Boscan, Cerro Negro, and Furrial samples.[28] In the present work, we also isolated the TC fractions present in the four asphaltene samples. Some properties and laser desorption ionization mass spectroscopy (LDIMS) of the TC fraction from Cerro Negro asphaltenes were reported.[6] These LDIMS values suggested that most of the TC fraction, soluble in *n*-heptane, was released from asphaltene during the A1 and A2

dx.doi.org/10.1021/ef3002857 | *Energy Fuels* 2012, 26, 4968−4977

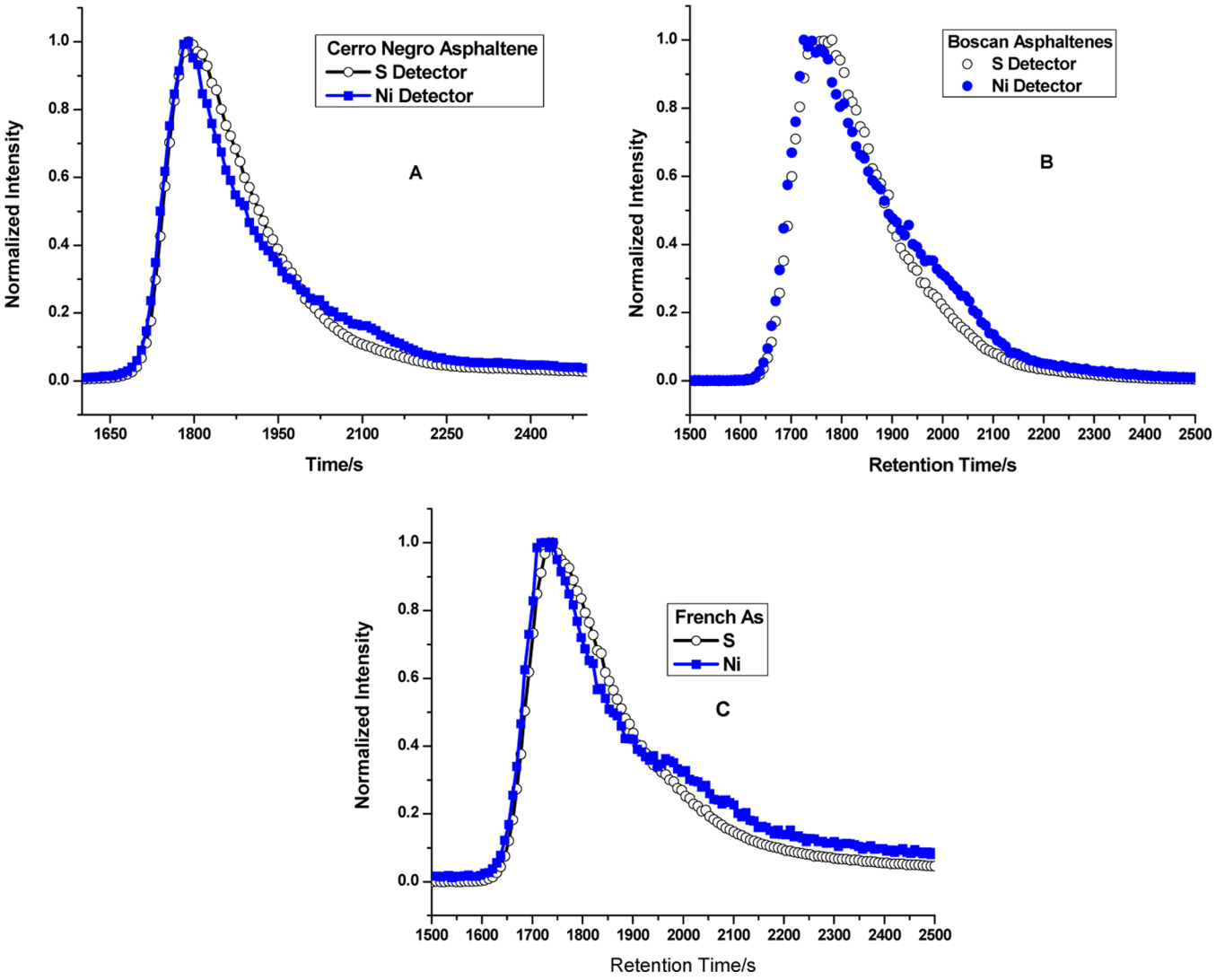

Figure 5. Comparison of normalized μSEC ICP profiles measured with S and Ni detectors for (A) Cerro Negro, (B) Boscan, (C) French. The interesting resemblance between sulfur and nickel in each case suggests that nickel compounds are trapped within asphaltene aggregates. Similar results were found for corresponding fractions A1 and A2 (not shown).

separation steps. A1 was the most abundant fraction in all the samples studied, except in the case of the French sample, which showed a low A1 yield (Table 2). This low A1 yield could be considered a preliminary result since reaction in this case was extremely slow (see the Experimental Section). Significant quantities of TCs were isolated in all cases, showing the high capacity of asphaltenes to trap external compounds.

The measured metal concentrations for Cerro Negro and Furrial samples are shown in Table 3. No significant differences between the Ni isotopes were found. This was a constant for all experiments performed in this work. As expected, vanadium and nickel showed the highest metal concentration values, with very small quantities of the other analyzed metals. Errors ranging from 5 to 10% were estimated for both nickel and vanadium, and the values for other metals were roughly estimated. Vanadium and nickel concentrations for the A1 and A2 fractions were unexpectedly high (about 10% higher than expected on mass balance grounds) because the work up required to process these fractions is likely to remove unaccounted material containing either low or zero quantities of these metals.

The percentage metal distribution, $\%M(i)$, among different fractions (A1, A2, and TC) was obtained from percentages (f_i, Table 2) and metal contents (M_i, Table 3), using eq 4:

$$\%M(i) = 100\frac{f_i M_i}{f_{A1}M_{A1} + f_{A2}M_{A2} + f_{TC}M_{TC}} \quad (4)$$

In this equation, the denominator is equal to the total quantity of metal present in 100 g of sample. $\%M(i)$ values for Cerro Negro and Furrial samples are shown in Table 4. The error propagation from this formula was calculated using 20% and 10% errors for f_i and M_i, respectively. This calculation led to errors of about 30%, 25%, and 20% for A1, A2, and TC determinations, respectively.

The results of $\%M(i)$ calculation are shown in Table 4. The isotopic average was employed in the case of nickel. Although the errors in the percentage distribution were noticeable, as a result of measurement uncertainty and error propagation, clear trends indicate that fraction A1 is predominant and that these metals selectively concentrate in fraction A1, in agreement with reported values.[29] The properties of the A1 and A2 fractions have been previously reported and discussed, and the reader is referred to the literature for further details.[6,28] The most distinct

dx.doi.org/10.1021/ef3002857 | *Energy Fuels* 2012, 26, 4968−4977

difference among these fractions is the lower solubility of A1 in many solvents,[19] particularly toluene, in which A1 is practically insoluble at room temperature (see the Experimental Section). The TC fraction is a heptane-soluble fraction, for which some details have been reported elsewhere.[6] This fraction, however, cannot be removed from asphaltenes by the usual heptane treatment (see the Experimental Section).

Normalized μSEC ICP profiles for asphaltenes and their fractions, recorded with a sulfur detector, are shown in Figures 1−4. Since sulfur should be present in all the asphaltene samples, a sulfur detector was considered to be a universal detector for asphaltenes.

The retention times for all the samples under study obtained using a sulfur detector are shown in Table 5. As can be seen, the retention times of asphaltene samples were all within about 100 s of each other. The relatively low value found for A2 in the Boscan sample was unexpected, although this finding will not be considered in this paper.

The normalized profiles for Cerro Negro asphaltene samples were almost identical, suggesting very similar hydrodynamic volumes and chemical compositions for the different fractions of this sample (Figure 1). Similar results were found for the French sample, which showed small differences in retention times (Figure 4). Profiles for Furrial were, however, quite different compared to those of the other samples, showing more tailing and a shift to longer retention times.

Figure 5 compares the normalized profiles for both sulfur and nickel for the Boscan, Cerro Negro, and French asphaltene samples. As can be seen, the profiles were very similar and overlapped for significant time intervals. Moreover, it is important to note that the nickel profiles matched the sulfur profiles in all cases, indicating that the corresponding nickel porphyrins do not present a singular profile of their own. Instead, their profile resembled that of the corresponding asphaltenes. Similar results were found for the A1 and A2 fractions (Figure 6). This close similarity is discussed below in terms of MPs being part of the asphaltene aggregates. In the case of the Furrial (Figure 7) sample, this resemblance was obtained for retention times shorter than that of the maximum, and the overlapping decreased in the order A1 > A2 > As (see the Discussion).

The vanadium and sulfur normalized profiles for the Boscan, Cerro Negro, and French asphaltenes are shown in Figure 8. Again, as was the case for nickel (Figure 5), the vanadium profiles followed or matched the sulfur profiles up to a point where the vanadium compounds were clearly differentiated from the sulfur profile. We suggest that this can be produced by the dissociation of some MP−asphaltene aggregates. The percentages of this detached vanadium were estimated using the procedure described above (see Table 6 and Methods), and in all cases this value was lower than about 30%. For the Furrial asphaltenes, the sulfur and vanadium profiles were quite different, and thus this method could not be used in this case. However, by comparison with the profiles in Figure 9, it can be inferred that the detached vanadium was very small in this case.

The profiles for the TC fraction corresponding to Boscan and Furrial are shown in Figure 10. A higher concentration of Furrial was needed to detect the very small amount of nickel present in this fraction (see Tables 1 and 3). The concentration of vanadyl porphyrins in this fraction was significant and could partly account for the Soret bands usually observed in these samples. Note that these profiles were not comparable to each other. Retention times for TC were higher than those of the corresponding asphaltene fractions (see Figures 1−3), probably as a result of their smaller hydrodynamic size. Since the TC fraction is not composed of asphaltenes, and thus is not expected to aggregate, the observed higher retention time could be anticipated.

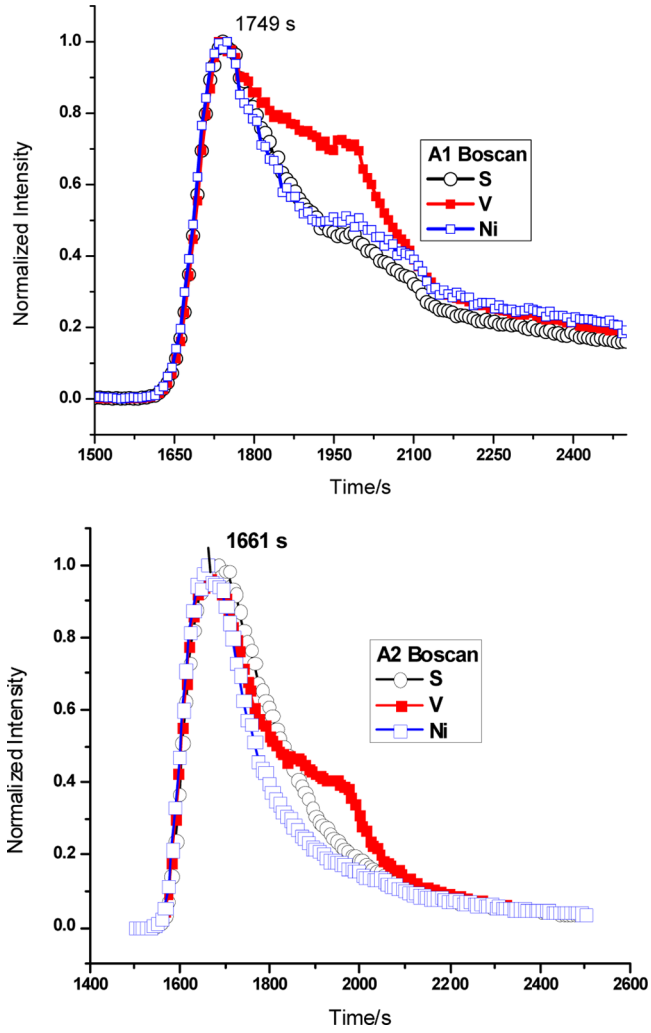

Figure 6. Normalized μSEC ICP profiles for sulfur, vanadium, and nickel measured for A1 (top) and A2 (bottom) fractions of Boscan asphaltenes. Note how the nickel profiles follow or match the sulfur profiles in both cases. For vanadium some detachment from the asphaltene profile is apparent.

DISCUSSION

The high capacity of asphaltenes to withhold or trap compounds is demonstrated by the significant quantities of TCs isolated from them (see Table 2). This fraction is composed of heptane-soluble compounds and, consequently, it does not contain asphaltenes. This can be seen by comparing the corresponding profiles (Figures 1−3). Very small quantities of MPs were found in the TC fraction (see Table 3 and Figure 10). This fact, along with the presence of large paraffins (MMs around 600),[6] showed that the housing voids (see below) can have large volumes and that trapping is not specific. A plausible explanation for this behavior is that aggregate penetration by TCs was followed by aggregate rearrangement, leading to interactions among asphaltene molecules (e.g., dispersion, polar, and hydrogen-bonding interactions). Hence, removal of the TCs from such structures (guest−host structures) would be equivalent to asphaltene

dx.doi.org/10.1021/ef3002857 | Energy Fuels 2012, 26, 4968−4977

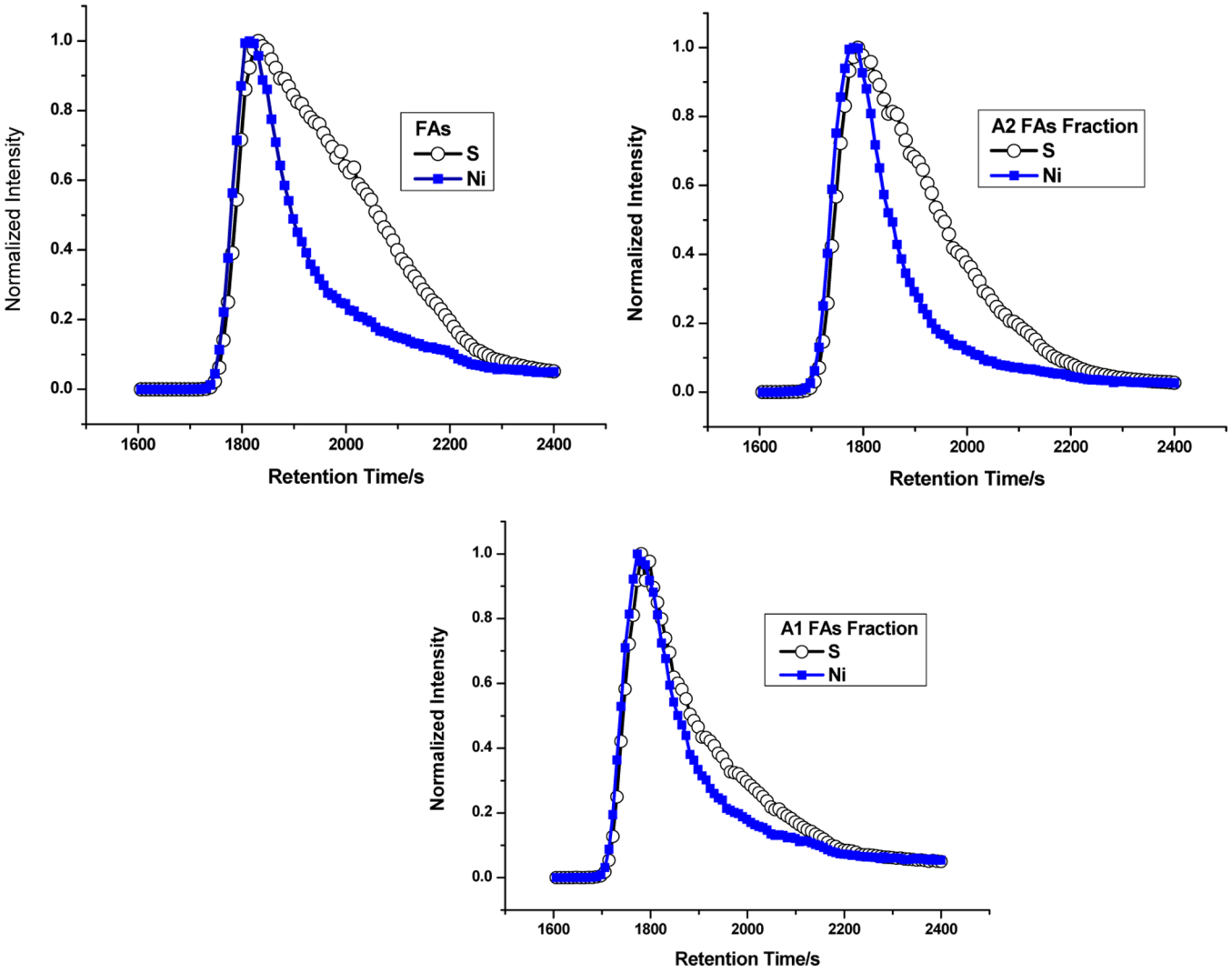

Figure 7. Comparison of normalized sulfur and nickel μSEC ICP profiles for Furrial samples: clockwise, asphaltenes; A2 fraction; A1 fraction. Percentage nickel areas in them are As, 63; A1, 87; and A2, 66. The differences in profiles appear to be the result of aggregation (see the text).

dissociation in solution and, as known, this is a difficult process in any solvent (see below).

The colloidal behavior of asphaltenes was analyzed in terms of fractal theory.[24,30] A property of fractals relevant to trapping reveals that these bodies cannot fill the entire space they are immersed in.[31] In other words, fractals contain voids or holes, which in the case of asphaltene colloids, would be spread randomly all over the body. These voids would of course be filled by media and would account for the TC fraction and for the very large amount of media (mostly resins) found when asphaltenes are separated from crude oils. This shows that occlusion or trapping is a consequence of "fractality". Another property of fractals is that their structure is scale independent, meaning, in our case, that random distributions of voids would be found at large (e.g., flocks) and small (e.g., aggregates or nanoaggregates) scales. This would account for irregular or random packing of the molecules forming the nanoaggregates.

As shown above, most MPs were found in asphaltenes and their fractions, and small (but significant) quantities of nickel and vanadium were detected in the TC fraction (see Table 4). We propose that MPs in asphaltenes enter and remain in the asphaltene matrix in the same way as described above for TCs. Accordingly, no specific bonding, such as hydrogen bonding or covalent bonding, is required to account for the presence of MPs in asphaltene aggregates.

As shown in Figures 5 and 6, the nickel profiles matched the sulfur profiles, indicating that nickel porphyrins do not have a specific profile. This could be easily explained in terms of the above MP-trapping approach. Extracting the MPs from these aggregates would require breaking several asphaltene bonds (e.g., dispersion, polar, and hydrogen bonds) and this could be a very difficult task.

In the case of the Furrial samples, the similarities between the sulfur and nickel profiles were partial, and they increased in the order asphaltene, A2, and A1, presumably as a result of an increase in aggregate concentration in the same order (Figure 7). Overlapping of the corresponding profiles up to the maximum and beyond is consistent with the above aggregation arguments.

The μSEC ICP profiles, obtained using a vanadium detector, showed a range of bands different from those measured for sulfur (Figure 8). We suggest that these bands register vanadyl porphyrins that dissociate from asphaltene aggregates either after immediate contact with the mobile phase (THF) or during sample transit within the column. An estimate of the relative quantity of vanadyl porphyrins dissociated (VD, see Table 6)

dx.doi.org/10.1021/ef3002857 | *Energy Fuels* 2012, 26, 4968–4977

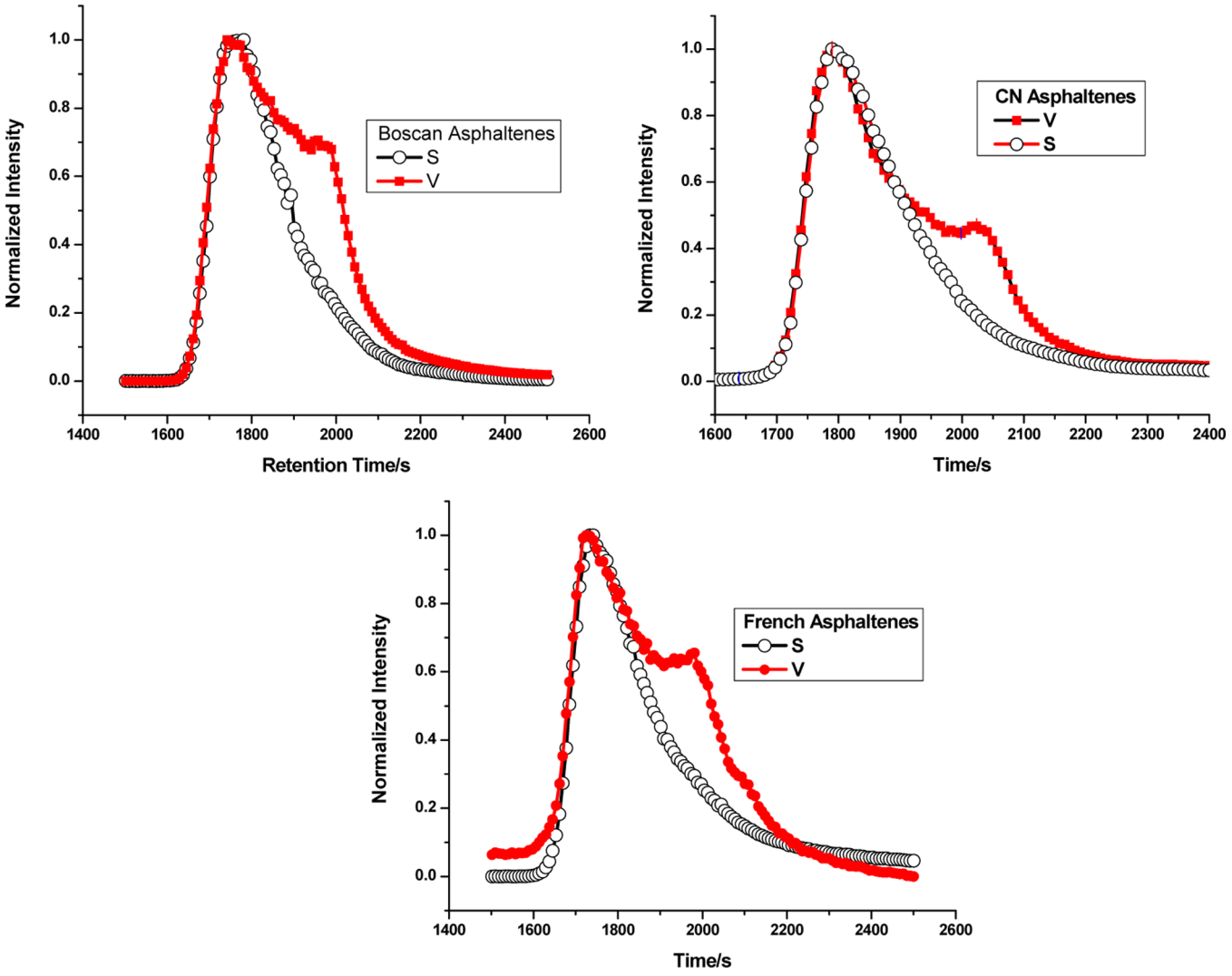

Figure 8. Comparison of normalized sulfur and vanadium μSEC ICP profiles for Boscan (top, left), Cerro Negro (top, right), and French asphaltenes (bottom); as was the case for nickel (Figure 5), vanadium profiles follow sulfur profiles up to a time where detachment occurs. Between 15 (Cerro Negro) and 30% (Boscan) of vanadium compounds was estimated to detach from asphaltenes during chromatography (see the text).

Table 6. Percentages of DV[a] Estimated by Area Comparison

ACN[b]	15
A1 CN	30
A2 CN	25
AB[c]	18
A1B	7
A2B	23
French As	23
French A1	9
French A2	19

[a]Vanadium dissociated from asphaltenes during μSEC run (see text and Methods). [b]Cerro Negro. [c]Boscan.

showed that most vanadyl porphyrins remained attached to asphaltenes.

It is interesting to note that although vanadyl porphyrins detached from asphaltenes in measurable quantities, nickel porphyrin detachment was not unambiguously observed. Freeman and co-workers reported a lower solubility of etio and octaethyl nickel porphyrins compared to the corresponding vanadyl compounds in various solvents (e.g., methylene chloride,

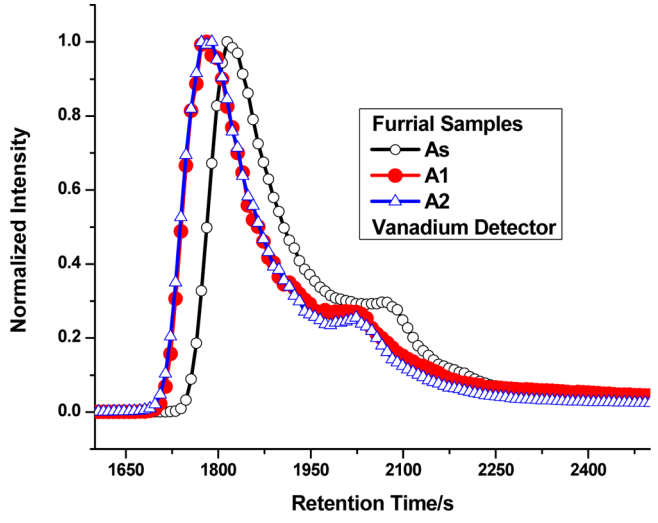

Figure 9. μSEC ICP profiles for Furrial samples recorded with a vanadium detector. Note that the percentage of detachment, as suggested by the shoulder in the bands, should be small and less than 15% .

dx.doi.org/10.1021/ef3002857 | *Energy Fuels* 2012, 26, 4968–4977

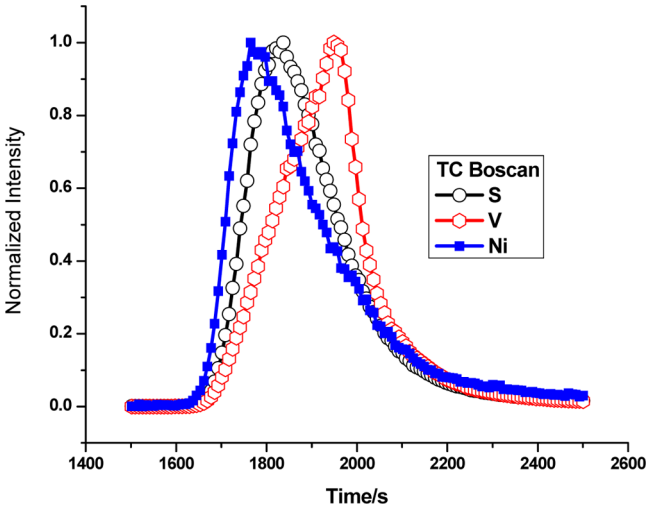

Figure 10. Comparison of sulfur, vanadium, and nickel μSEC ICP profiles measured for the TC fraction from Boscan. Similar results were obtained for Furrial and Cerro Negro samples.

ethyl acetate, acetonitrile, cyclohexane, ethanol, hexane, and methanol).[32] Thus, solubility may play an important role in explaining the above differences.

Using VPO, high temperature, and a good solvent (e.g., chloroform, *o*-dichlorobenzene,[20] and nitrobenzene,[21] see the Introduction), we reported that both the A1 and A2 fractions had aggregation trends, and these were higher for A1. High M_n values were reported for asphaltenes using both pyridine[25] and THF[21] (see the Introduction). In particular, when measured in THF, M_n values >4000 g mol^{-1} were found for Cerro Negro and other asphaltene samples. Thus, asphaltene aggregation in solution under usual laboratory conditions should always be expected. Thus, the resistance of MPs to solvent extraction can be explained by the fact that they are part of such asphaltene aggregates.

CONCLUSIONS AND FINAL REMARKS

The μSEC ICP results described herein show that both nickel and vanadyl porphyrin profiles match the sulfur profiles across significant time ranges, suggesting that these compounds are intercalated or trapped within asphaltene aggregates. This match was also found in profiles of A1 and A2, suggesting aggregate formation in both these asphaltene fractions.

The issues encountered during solvent extraction of metal porphyrins were related to the difficulties in breaking asphaltenes aggregates apart, regardless of the solvent used. The relatively high quantities of TCs isolated demonstrate the high capacity of asphaltenes to trap external compounds.

The trapping of MPs is a particular case of a more general trapping of compounds (TCs) by asphaltene aggregates. Because compounds such as paraffin, resins, and MPs have been found in these TCs, such trapping is not specific. Thus, as proposed above, trapping is the result of filling fractal voids with media components of all sorts. Small but significant quantities of both nickel and vanadyl porphyrins were detected in the TCs. Moreover, void volumes were large enough to include these MPs. This means that no specific interactions between MPs and asphaltenes are required for them to be trapped within the aggregates. As described above, asphaltene nanoaggregates in solution are expected to have a number of molecules large enough to contain intercalated MPs.

AUTHOR INFORMATION

Corresponding Author

*E-mail: soaceved@cantv.net.

Notes

The authors declare no competing financial interest.

ACKNOWLEDGMENTS

Financial support by the following institutions and programs is gratefully acknowledged: the French-Venezuelan PCP Program; the CDCH-UCV, Project PG 03-7779-2009-1; and FONACIT, Project PG 2005000430. S.A. thanks Lic. Betilde Segovia for administrative assistance.

NOMENCLATURE

A1 = fraction isolated from asphaltenes using the *p*-nitro phenol (PNP) method described above. The more relevant characteristic of A1 is its very low solubility in toluene (around 90 mg L^{-1}, room conditions). Because it is part of the asphaltenes, this fraction should be solubilized by other components of the asphaltenes (A2, TC) resulting in soluble aggregates. This issue has been extensively discussed in the literature.[6,28]

A2 = another fraction isolated from asphaltenes using the PNP method. It has a solubility similar to asphaltenes, and it have been proposed that this fraction forms soluble aggregates with A1[6,28]

As = asphaltenes

APPI = atmospheric pressure photo ionization mass spectrometry method

B = Boscan

CN = Cerro Negro

DBE = double bond equivalent: number equal to the number of double bonds plus number of rings in any molecular structure

DPEP = deoxophylloerythroetioporphyrin, a porphyrine structure. Examples of these and others could be found in ref 12.

DV = detached vanadium; vanadium MP detached from asphaltene aggregates during transit of sample within the SEC column

EIMS = electron ionization mass spectrometry

EXAFS = extended X-rays absorption fine structure spectroscopy

f = percentage of fraction

FTICR MS = Fourier transform ion cyclotron resonance mass spectrometry

μFI = microflow injection

ICP = inductively coupled plasma detector

LDIMS = laser desorption ionization mass spectrometry

m = mass of substance

M_i = metal content (V or Ni) in a particular fraction (i = A1, A2, TC)

% $M(i)$ = distribution of metals among fractions A1, A2, and TC

MM = molecular mass

M_n = number average molecular mass, often called number average molecular weight

MPs = metallic porphyrins

MS = mass spectrometry

PDVSA = Venezuelan oil company

PNP = *p*-nitro phenol method; used to fractionate asphaltenes in fractions A1, A2, and TC

dx.doi.org/10.1021/ef3002857 | *Energy Fuels* 2012, 26, 4968−4977

R = percentage of sample recovery during fractionation of asphaltenes
RED = relative energy difference; a parameter related to solubility and solubility parameter difference
μ-SEC-HR ICP MS = liquid chromatography technique coupled to a mass spectrometer with an ICP detector
TC = trapped compounds; compounds found in asphaltenes and separated from them using the PNP method. These are soluble in *n*-heptane and contain paraffin, resins, and MP. Here we propose that they fill voids in the fractal structure of asphaltene aggregates (see above)
THF = tetrahydrofuran
VO (II) = vanadyl group in vanadyl porphyrins
XANES = X-ray absorption near edge spectroscopy
Z-number = negative even number associated with the number of double bond equivalents (DBE) in a molecular structure

REFERENCES

(1) Dechaine, G. P.; Gray, M. R. *Energy Fuels* **2010**, *24*, 2795−2808.
(2) Erdman, J. G.; Harju, P. H. *J. Chem. Eng. Data* **1963**, *8*, 252−258.
(3) Mujica, V.; Nieto, P.; Puerta, L.; Acevedo, S. *Energy Fuels* **2000**, *14*, 632−639.
(4) Liao, Z.; Geng, A.; Graciaa, A.; Creux, P.; Chrostowska, A.; Zhang, Y. *Energy Fuels* **2006**, *20*, 1131−1136.
(5) Liao, Z.; Zhou, H.; Graciaa, A.; Chrostowska, A.; Creux, P.; Geng, A. *Energy Fuels* **2005**, *19* (1), 180−186.
(6) Acevedo, S.; Cordero, T., J. M.; Carrier, H.; Bouyssiere, B.; Lobinski, R. *Energy Fuels* **2009**, *23* (2), 842−848.
(7) Gray, M. R.; Tykwinski, R. R.; Stryker, J. M.; Xiaoli, T. *Energy Fuels* **2011**, *25*, 3125−3134.
(8) Van Berkel, G. J.; Quirke, J. M. E.; Filby, R. H. *Org. Geochem.* **1989**, *14* (8), 119−129.
(9) Van Berkel, G. J.; Quirke, J. M. E.; Filby, R. H. *Org. Geochem.* **1989**, *14*, 130−145.
(10) Beato, B. D.; Yost, R. A.; Van Berkel, G. J.; Filby, R. H.; Quirke, J. M. E. *Org. Geochem.* **1991**, *17*, 93−105.
(11) Qian, K.; Mennito, A. S.; Edwards, K. E.; Ferrughelli, D. T. *Rapid Commun. Mass Spectrom.* **2008**, *22*, 2153.
(12) Qian, K.; Edwards, K. E.; Mennito, A. S.; Walters, C. C.; Kushnerick, J. D. *Anal. Chem.* **2010**, *82*, 413−419.
(13) Grigsby, R. D.; Green, J. B. *Energy Fuels* **1997**, *11*, 602−609.
(14) Goulon, J.; Retournard, A.; Friant, P.; Goulonginet, C.; Berthe, C.; Muller, J. F.; Poncet, J. L.; Guilard, R.; Escalier, J. C.; Neff, B. *J. Chem. Soc. Dalton* **1984**, 1095−1103.
(15) Miller, J. T.; Fisher, R. B.; van der Eerden, A. M. J.; Koningsberger, D. C. *Energy Fuels* **1999**, *13* (3), 719−727.
(16) McKenna, A. M.; Purcell, J. M.; Rodgers, R. P.; Marshall, A. G. *Energy Fuels* **2009**, *23*, 2122−2128.
(17) Yin, C. X.; Tan, X.; Klaus, M.; Stryker, J. M.; Gray, M. R. *Energy Fuels* **2008**, *22*, 2465−2469.
(18) Stoyanov, S. R.; Yin, C. X.; Gray, M. R.; Stryker, J. M.; Gusarov, S.; Kovalenko, A. J. *Phys. Chem. B* **2010**, *114*, 2180−2188.
(19) Acevedo, S.; Castro, A.; Vásquez, E.; Marcano, F.; Ranaudo, M. A. *Energy Fuels* **2010**, *24*, 5921−5933.
(20) Acevedo, S.; Guzmán, K.; Ocanto, O. *Energy Fuels* **2010**, *24*, 1809−1812.
(21) Acevedo, S.; Escobar, G.; Gutiérrez, L. B.; D'Aquino, J. A. *Fuel* **1991**, *71*, 1077−1079.
(22) Pomerantz, A. E.; Hammond, M. R.; Morrow, A. L.; Mullins, O. C.; Zare, R. N. *J. Am. Chem. Soc.* **2008**, *130*, 7216−7217.
(23) Martínez-Haya, B.; Hortal, A. R.; Hurtado, P. M.; Lobato, M. D.; Pedrosa, J. M. *J. Mass Spetrom* **2007**, *42*, 701.
(24) Sheu, E. Y. *Structures and Dynamics of Asphaltenes*; Mullins, O. C., Sheu, E. Y., Eds.; Plenum Press: New York, 1998; Chapter IV, pp 115 − 144.
(25) Acevedo, S.; Layrisse, I.; Méndez, B.; Rivas, H.; Rojas, A. *Fuel* **1985**, *64*, 1741.
(26) Pohl, P.; Dural, J.; Vorapalawut, N.; Merdrignac, I.; Lienemann, C. P.; Carrier, H.; Grassl, B.; Bouyssiere, B.; Lobinski, R. *J. Anal. At. Spectrom.* **2010**, *25*, 1974−1977.
(27) Caumette, G.; Lienemann, C. P.; Merdrignac, I.; Paucot, H.; Bouyssiere, B.; Lobinski, R. *Talanta* **2009**, *80*, 1039.
(28) Gutiérrez, L. B.; Ranaudo, M. A.; Méndez, B.; Acevedo, S. *Energy Fuels* **2001**, *15*, 624−628.
(29) Marcano, F.; Flores, R.; Chirinos, J.; Ranaudo, M. A. *Energy Fuels* **2011**, *25*, 2137−2141.
(30) Sirota, E. B.; Lin, M. Y. *Energy Fuels* **2007**, *21*, 2809−2815.
(31) Vicsek, T. *Fractal Grow Phenomena*, 2nd ed.; World Scientific Publishing: Singapore, 1992; Chapter 2.
(32) Freeman, D. H.; Swahn, I. D.; Hambright, P. *Energy Fuels* **1990**, *4*, 699−704.